4-2018

Evaluation of Beam Quality Study of Arbitrary Beam Profiles from On-Wafer Vertical Cavity Surface Emitting Lasers

Joshua D. Tate
United States Military Academy

Joshua B. Groen
United States Military Academy

Kirk A. Ingold
United States Military Academy

James J. Raftery Jr.
United States Military Academy

Proceedings of The National Conference
On Undergraduate Research (NCUR) 2018
University of Central Oklahoma
Edmond, Oklahoma
April 5-7, 2018

Evaluation of Beam Quality Study of Arbitrary Beam Profiles from On-Wafer Vertical Cavity Surface Emitting Lasers

Joshua Tate
Electrical Engineering
United States Military Academy
West Point, New York 10996 USA

Faculty Advisors: Dr. Kirk Ingold, Dr. James Raftery, Joshua Groen

Abstract

Vertical cavity surface emitting lasers (VCSELs) have found mainstream use in data centers and short-haul optical fiber communications. Along with the increase in the capacity of such systems comes an increase in the demand for greater power efficiency. System evaluation now includes an assessment of the energy required for each bit of data, a metric referred to as 'joules per bit'. One source of loss for VCSELs is coupling loss, which is due to a mismatch in the mode profiles of the VCSELs and the optical fiber into which the VSCEL light is coupled. One way to reduce this loss is to develop single-mode VCSEL devices that are modally matched to optical fiber. Efficient development of these devices requires a technique for rapidly evaluating beam quality. This study investigates the use of a vertically mounted commercial beam profiling system and hardware interface software to quickly evaluate the beam quality of arbitrary beam profiles from on-wafer mounted VCSEL devices. This system captures the beam profile emitted from a VCSEL device at fixed locations along the vertical axis. Each image is evaluated within software along a predetermined axis, and the beam quality, or M2, is calculated according to international standards. This system is quantitatively compared against a commercial software package designed for determining beam quality across a fixed axis.

Keywords: Vertical Cavity Surface Emitting Laser, Beam Quality Propagation Factor, Second Moment Calculation

1. Introduction

This study explores a novel method for assessing the beam quality propagation factor of vertical cavity surface emitting lasers (VCSELs). As the demand for high-speed data interconnects increases, so too has the demand for effective methods of data transmission through optical means.[1] Optical interconnects provide uniquely wide system bandwidth, immunity to electrostatic interference and crosstalk, lower signal attenuation rates, and reduced safety risks.[2] Using a VCSEL as the light source in optical communications systems has several advantages. VCSELs are small in size, their optical apertures typically being less than 10 µm in diameter. In addition to the spatial benefits conferred by the VCSEL's size, the exceptionally small VCSEL architecture allows for a single-mode optical output. The length of the lasing cavity is such that the frequency spacing of longitudinal modes more easily allows for the isolation of a single mode when gain is applied.[3] Having a single-mode output is ideal for high-speed optical communications because it alleviates the problem of intermodal dispersion, which can distort data as it propagates along an optical transmission line.[4] Given that VCSEL emitters are typically coupled into optical fiber, signal attenuation due to coupling loss becomes a concern. One cause of coupling loss is modal mismatch, which can be induced by a transmission source with a low beam quality. Therefore, it is important to have a reliable, comprehensive, and precise method of assessing the beam quality of VCSEL devices.[5]

Beam quality is a measure of how closely a device's optical output resembles the ideal Gaussian beam profile. A widely used metric for quantifying beam quality propagation factor is the M^2 factor. The M^2 factor uses the beam's waist size and divergence angle to determine how closely that beam resembles an ideal Gaussian beam. Graphical representation of beam waist and divergence angle are depicted in Figure 1, where the *z* axis is the axis of propagation.

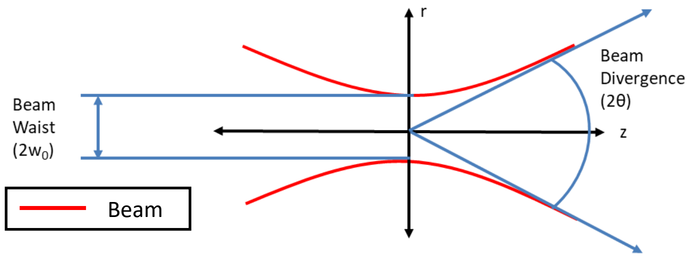

Figure 1. Graphical representation of beam waist ($2w_0$) and divergence angle (2θ).

M^2 is calculated according to equation (1) using the beam waist $2w_0$, divergence angle 2θ, and optical wavelength λ.[6]

$$M^2 = \frac{(2w_0)(2\theta)}{4\lambda\pi} \quad (1)$$

The International Organization for Standardization specifies the standard for capturing beam data and calculating M^2 in ISO #11146-1.[7] The standard defines methods for capturing the beam profile, calculating the beam waist and divergence, and approximating the M^2. These methods are employed in this study for evaluating M^2.

Current methods of measuring M^2 offer a limited picture of beam quality. Experimental testing conducted prior to and during this study indicates that M^2 results vary according to the angular orientation of VCSEL devices in measurement systems.[8] Figure 2 shows the effect of a device's rotational orientation on its measured M^2 value. Assessing a device's M^2 value with respect to only one physical orientation can be misleading when one is attempting to fully characterize a particular device. The core proposition of this study is that by mimicking physical rotation using software, a consistent M^2 range can be produced for a particular VCSEL that is independent of that device's rotational orientation in the measurement system.

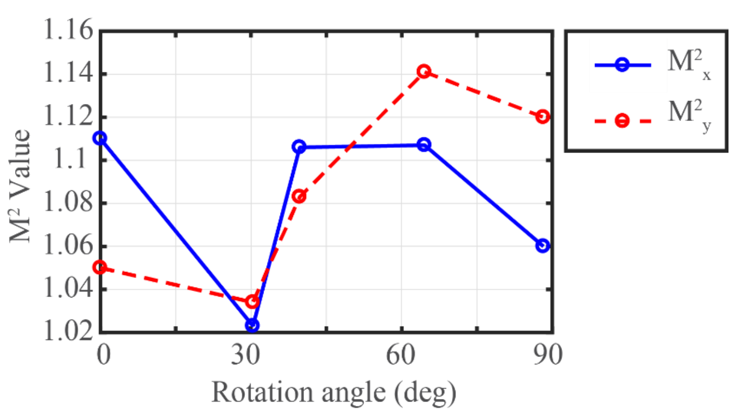

Figure 2. M^2 measurements for a VCSEL over a range of physical rotational orientations

2. Methodology

By iteratively rotating captured beam profiles in software and calculating M^2 for each iteration, a range of M^2 values can be produced such that possible variations due to a device's rotational orientation would be represented. Should this calculation method adequately account for all sources of variation in M^2 measurement, it would offer a consistent, comprehensive representation of beam quality independent of a device's angular orientation. This is because the source of variation will have been accounted for in software.

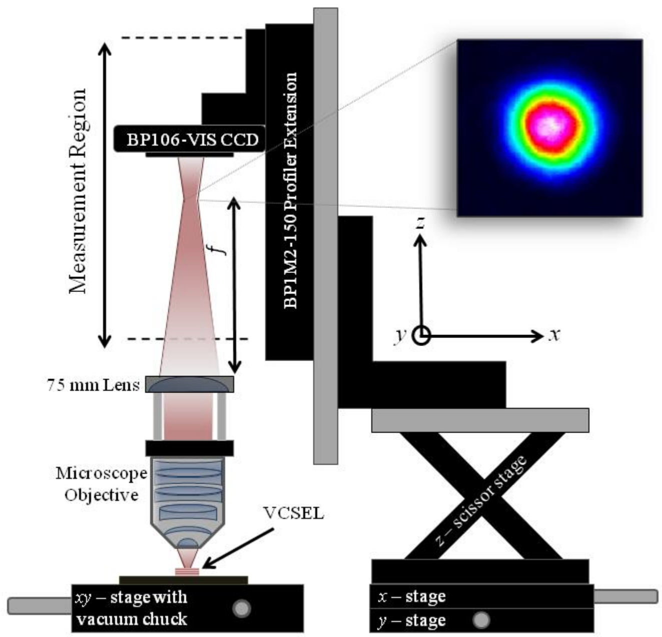

Figure 2. Beam profiling hardware system[9]

Previous work by Blane, et al, established a system for capturing the beam profile of on-wafer VCSEL devices. [9] Figure 2 shows a diagram of the beam profiling hardware system used in this study. It features a CCD camera fixed to an automated, movable stage. The camera captures cross sections of beam intensity profiles at various distances along the beam's axis of propagation. The commercial software accompanying the hardware system was used to control the movable stage. In accordance with ISO #11146-1, the second-moment method was used to calculate the widths of the beam cross-sections captured by the beam profiler. Beam waist, beam divergence, and ultimately M^2 were determined using these beam widths. MATLAB was used to perform this calculation as well as perform a virtual rotation of beam data in order to capture a range of possible M^2 values. M^2 results from the commercial software were used as the standard of accuracy in developing the MATLAB software used in this study. MATLAB results typically fell within a margin of error sufficient to meet the intent of this study.

The procedure for data capture involved capturing the beam profile of a particular device at various physical rotational orientations within the measurement system. For each iteration, the VCSEL wafer was manually rotated and the beam profile captured through the measurement region of the system (e.g. $0 < z < 150$mm). The precise device orientation was determined retroactively using digitization software on microscope photographs of the VCSELs. Additionally, great care was taken to minimize additional variables that could affect the beam profile measurements as the physical orientation of the VCSEL changed. One example was the consistent placement of the probe used to supply pump current to the devices. Given that current density can vary throughout a particular device, it was important to ensure that the probe tip was placed in roughly the same spot for each rotational iteration of measurement. Figure 3 summarizes the data acquisition and calculation procedure.

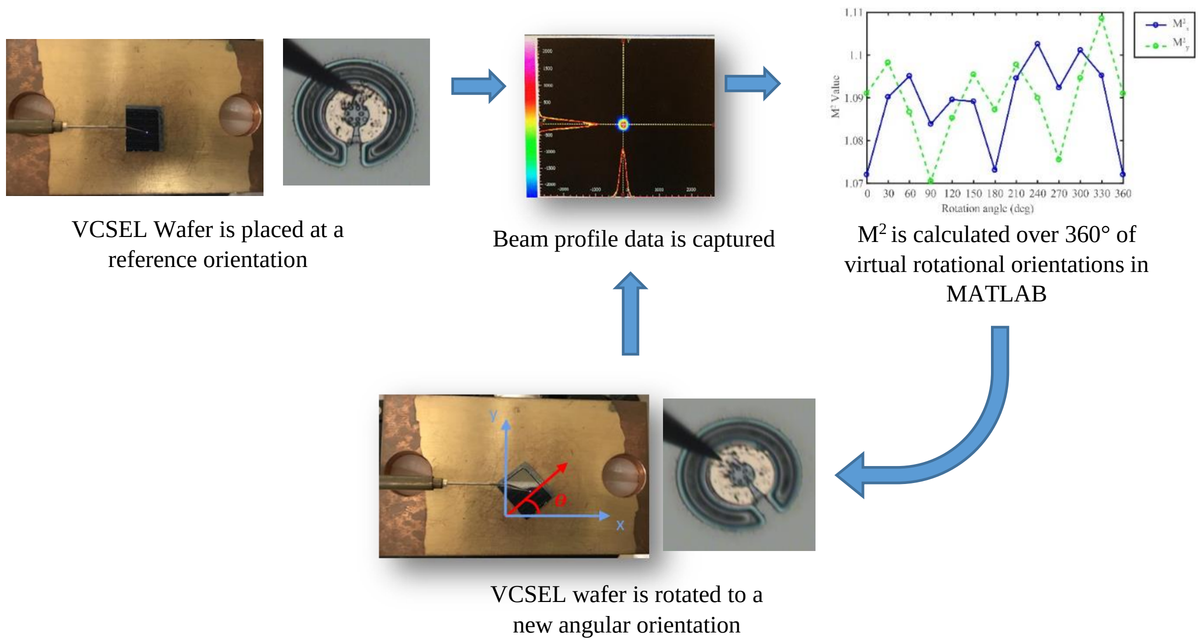

Figure 3. Experimental procedure for characterizing a single device over a range of physical orientations.

Figure 4 depicts the result of applying the software rotation algorithm to a particular beam profile cross-section. Such rotation is applied to all cross-sections captured for a particular measurement iteration. The angle of physical rotation is reported with respect to the initial reference orientation and is referred to as θ while the angle of virtual rotation applied by software is referred to as φ. For each virtual rotation angle, the beam diameter was calculated using the second moment methods defined in the ISO standard. The experimental procedure was conducted for two different VCSELs, one single-mode VCSEL and one multi-mode VCSEL. Evaluating two different devices tested the efficacy of the proposed beam evaluation for drastically different output characteristics. The single-mode device was pumped with 7mA of current while the multi-mode device was pumped with 5mA of current.

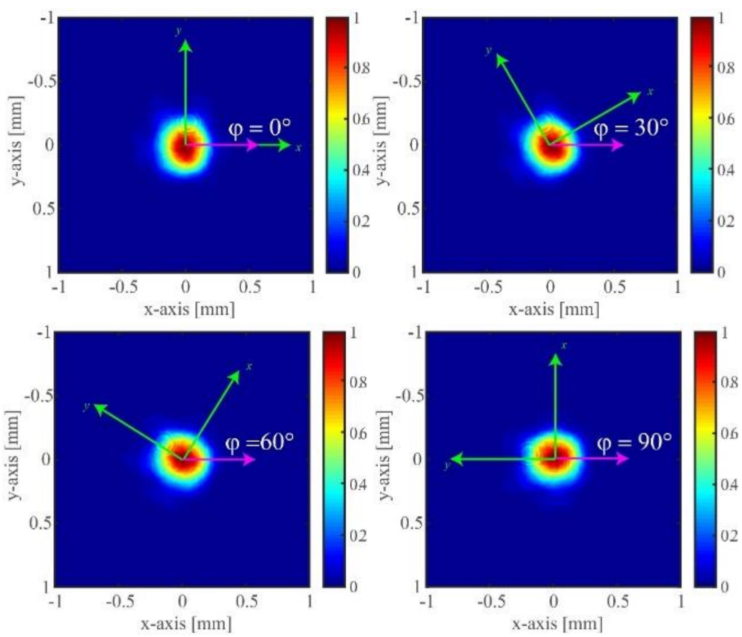

Figure 4. Beam profile cross-section at varying degrees of software rotation.

3. Results

The initial tests evaluated the M^2 of a single-mode and multi-mode VCSEL for a fixed virtual angle, $\varphi = 0°$, while rotating the physical angle from 0° to 90°. Images of the physically rotated devices are shown in Figures 5 and 7. These tests were performed to verify the proposition that the M^2 value of a device tends to vary as the rotational orientation of that device varies. This also serves to establish the range of M^2 values that the software rotation procedure is intended to capture. The calculated M^2 values for the single-mode and multi-mode devices are shown in Figures 6 and 8, respectively.

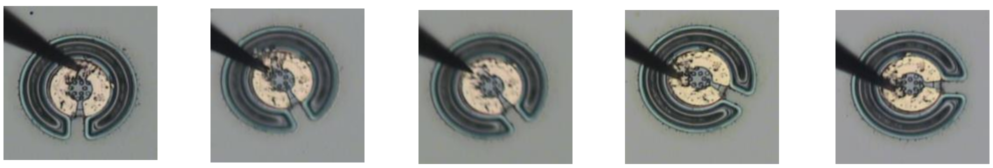

$\theta = 0°$ $\theta = 30.4°$ $\theta = 39.7°$ $\theta = 64.6°$ $\theta = 88.2°$

Figure 5. Microscope images of photonic crystal VCSEL at each angle θ

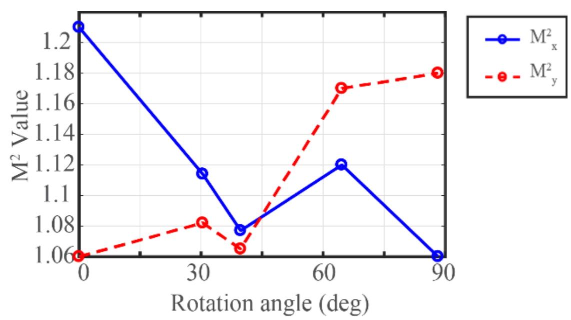

Figure 6. M^2 for θ values assumed by the single-mode VCSEL pumped with 7mA of current

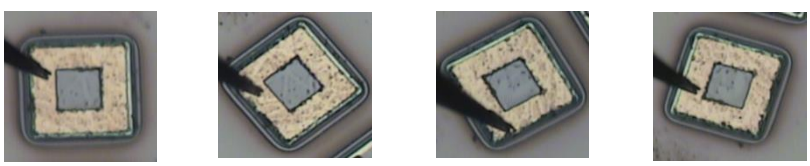

$\theta = 0°$ $\theta = 37.5°$ $\theta = -65.7°$ $\theta = -20.7°$

Figure 7. Microscope images of oxide-confined VCSEL at each angle θ

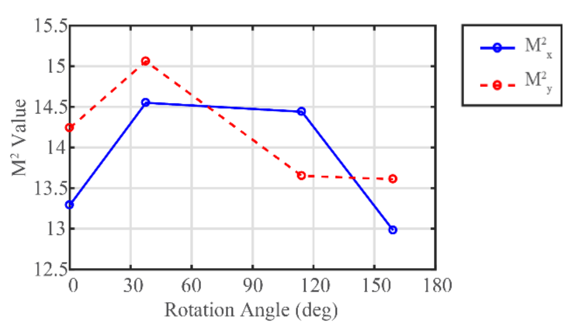

Figure 8. M^2 for all θ values assumed by the multi-mode VCSEL pumped with 5mA of current

As expected, the M^2 changes as the physical orientation of the VCSEL is rotated as shown in Figures 6 and 8. It is important to note in Figure 6, the M^2_x and M^2_y flip near 45°. This is expected, given that after 90°, the *x*- and *y*-axis of the VCSEL have flipped. Likewise, the range of M^2 are roughly the same at 0° and 90° for this device. These trends are not consistent for the multi-mode devices and may be due to the fact that the M^2 is much greater than 1 for this device. Note for each of the devices evaluated in Figures 5 and 7, the probe tip was placed at roughly the same location on the top contact, to minimize any variations in the current density.

The second set of tests conducted compared the range of calculated M^2 for a single-mode and multi-mode device. For each physical orientation θ, the M^2 was calculated at the range of angles, φ, from 0° to 360° at 30° increments. In Figures 9 and 10, the images of the device with the probe tip location is shown with the associated M^2 calculations.

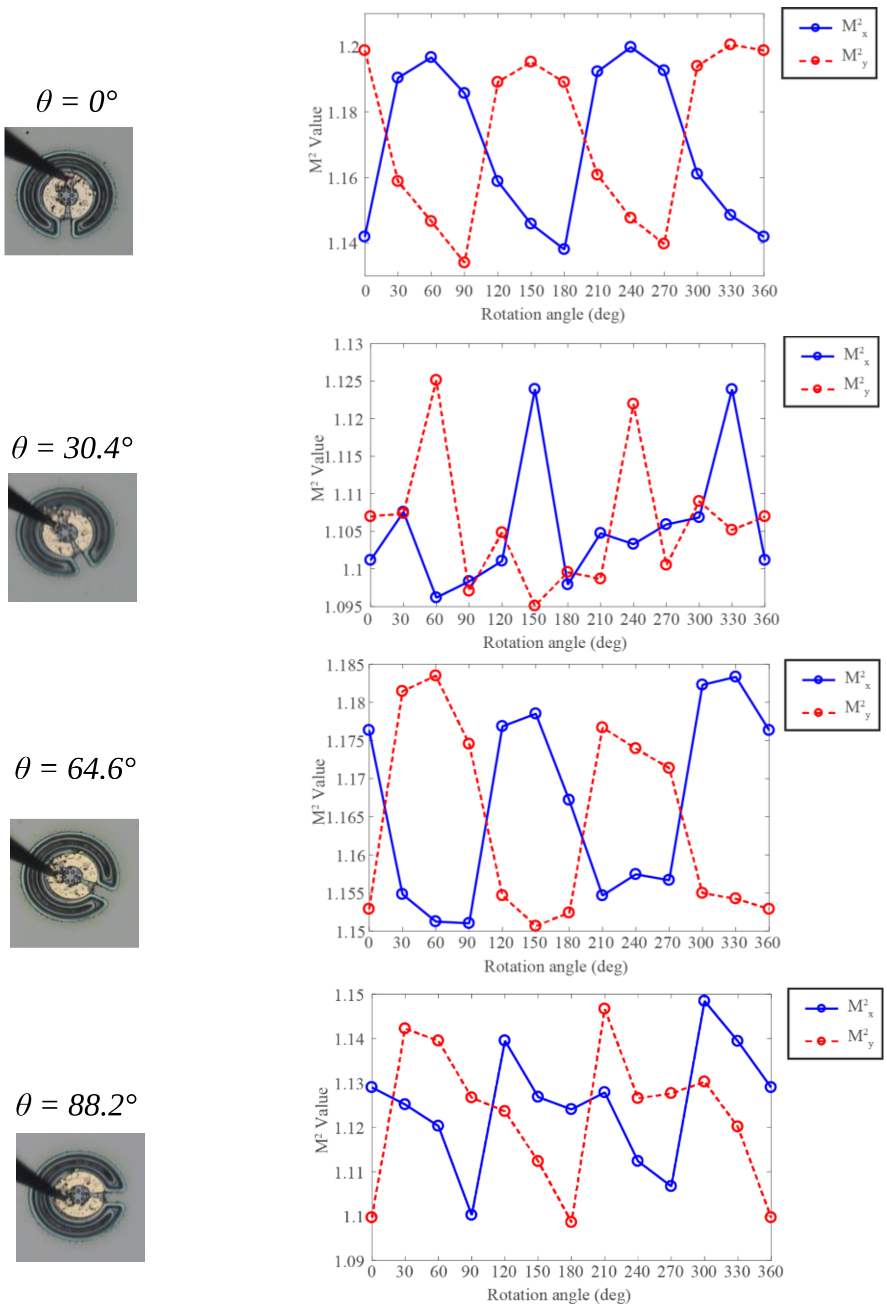

Figure 9. Rotation about φ for four physically rotated single-mode photonic crystal VCSEL devices.

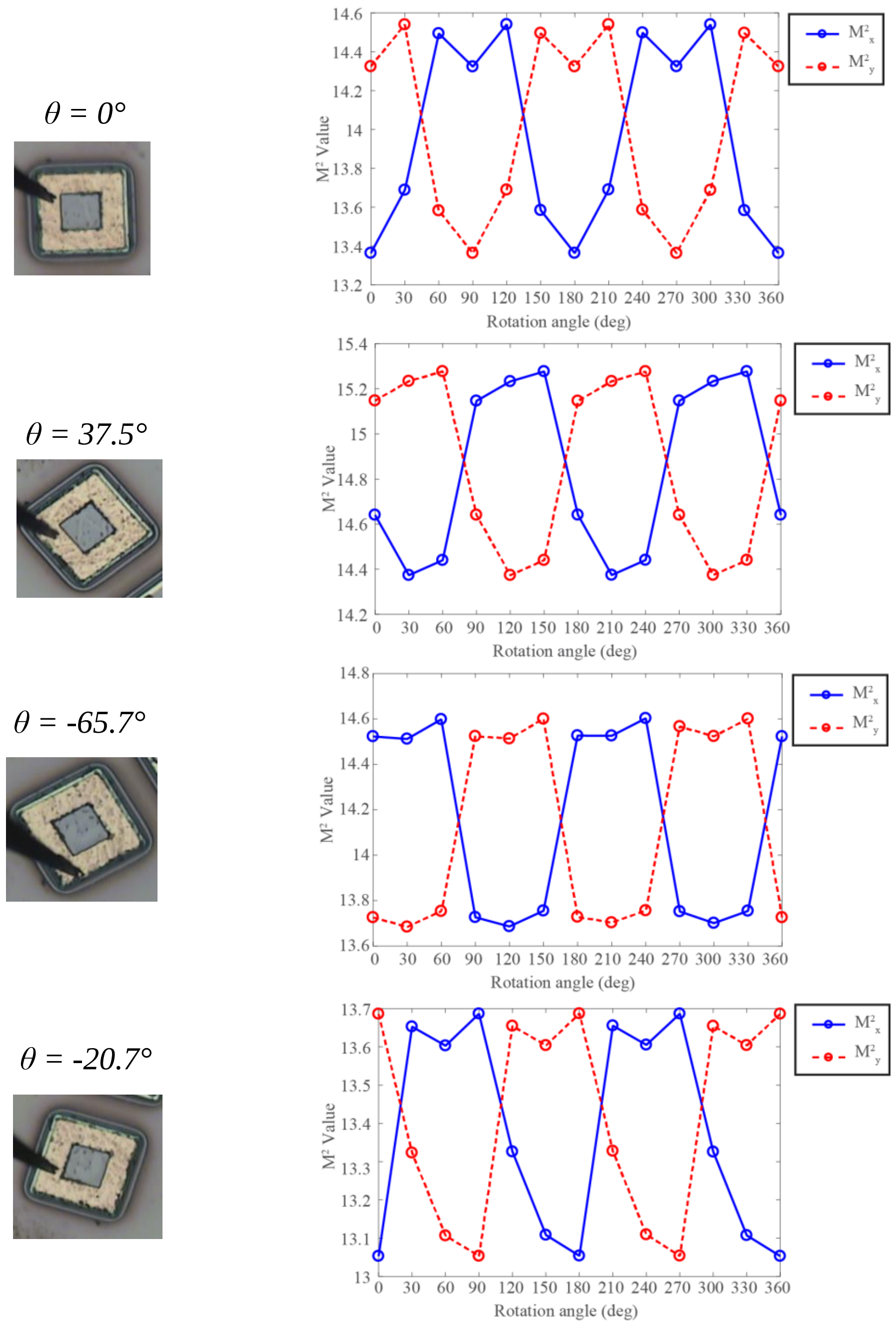

Figure 10. Rotation about φ for four physically rotated multi-mode oxide confined VCSEL devices.

As shown in Figures 9 and 10, a range of M^2 values are calculated for different physical orientations of the devices. As the virtual angle, φ, is changed in the software, the periodic nature of the M^2 calculations become apparent. In the mutli-mode calculations, the periodic structure is actually mapped to the physical rotations. As an example, between $\theta = 0°$ and $\theta = 37.5°$, there is a roughly 30° to 40° shift in the peak of the similar curves. This follows for the other two physical orientations as well. The results are not as apparent for the single-mode devices. This is a result of the near Gaussian, or $M^2 \approx 1$, beam calculations. Due to the finite pixel size of the CCD camera, the beam quality factor is more susceptible to quantization errors. The periodic structure is still visible, but not as useful as in the multi-mode calculations. Overall, these figures show the range of M^2 calculated for the physically rotated devices.

4. Conclusion

The vision for this study was to capture the full range of possible M^2 values for a particular device regardless of its rotational orientation. Based on the results, the proposed method of M^2 calculation was only able to account for some of the M^2 variation seen when changing the rotational orientation of VCSEL devices. The range of M^2 values calculated from physically rotating devices was typically larger than the range proposed by software rotation. Additionally, it is being assumed that the only significant source of variation for M^2 across iterations of physical rotation is that rotation itself. Should this assumption be incorrect, the M^2 range calculation would be unable to account for all present sources of variation. In theory, one would expect a software rotation to have the same effect as a physical device rotation, thus producing identical M^2 ranges for each physical device orientation. Therefore, more work needs to be done to ensure that no extraneous variables affect the beam characterization. The results, however, do make a strong case that current commercial methods of measuring M^2 offer an incomplete analysis of beam quality. They also show a promising step toward circumventing that problem.

5. Acknowledgements

The author wishes to express his appreciation to Professor K. D. Choquette and the University of Illinois-Urbana-Champaign for providing insight and the devices used for testing, as well as the Army Research Officer for providing funding for this study.

6. References

1. J. T. Blane, W. K. North, P. R. Zeidler, J. B. Dencker, D. B. Chacko, B. Souhan, K. A. Ingold, J. J. Raftery, "Beam quality study for single-mode oxide-confined and photonic crystal VCSELs," Proc. SPIE 9766, Vertical-Cavity Surface-Emitting Lasers XX, 97660I (4 March 2016); p.97660I, 2016.
2. J. S. Beasley, G. M. Miller, Modern electronic communication, 9th ed. (Upper Saddle River, NJ: Pearson Prentice Hall, 2008), 856-857.
3. Gerd Keiser, Optical fiber communications, 4th ed. (Boston: McGraw-Hill, 2000), 214.
4. Ibid., 70.
5. K. A. Ingold, J. D. Tate, B. E. Souhan, and J. J. Raftery, "Beam Quality Factor Analysis of On-Wafer Vertical Cavity Surface Emitting Lasers," in Conference on Lasers and Electro-Optics, OSA Technical Digest (online) (Optical Society of America, 2018), paper AW4O.3.
6. Bahaa Saleh, M. C. Teich, Fundamentals of photonics, 2nd ed. (Hoboken, NJ: Wiley-Interscience, 2009), 85.
7. ISO Standard 11146, “Lasers and laser-related equipment test methods for laser beam widths, divergence angles and beam propagation ratios.” 2005.
8. Ingold et al., “Beam Quality Factor Analysis of On-Wafer Vertical Cavity Surface Emitting Lasers.”
9. Ibid.